Reprinted From

THE
SHOCK AND VIBRATION
BULLETIN

Part 1
Keynote Address, Invited Papers
Damping and Isolation, Fluid-
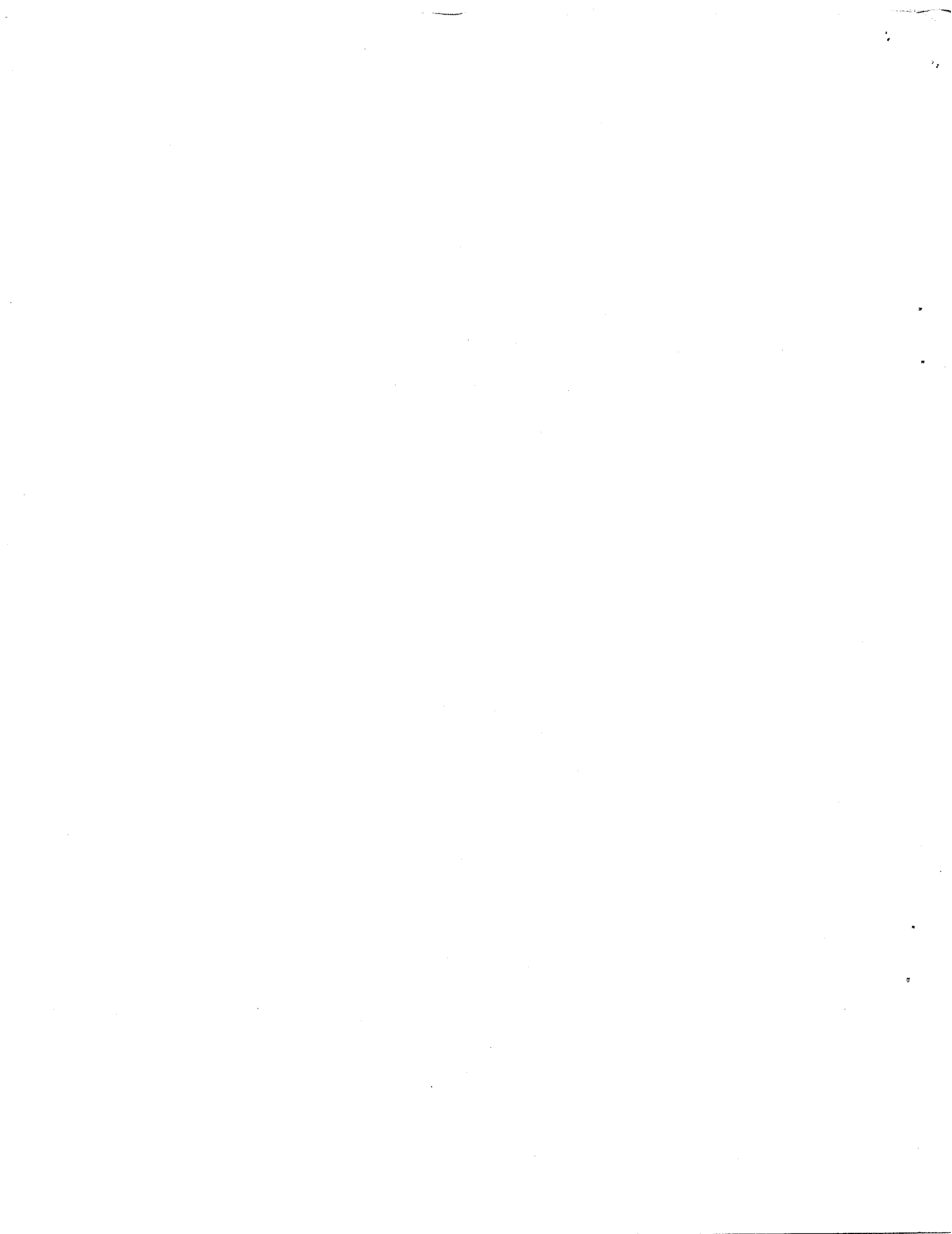### Structure Interaction

MAY 1981

A Publication of
**THE SHOCK AND VIBRATION
INFORMATION CENTER**
Naval Research Laboratory, Washington, D.C.

**Office of
The Under Secretary of Defense
for Research and Engineering**

SIMILITUDE ANALYSIS AND TESTING OF PROTOTYPE AND

1:13.8 SCALE MODEL OF AN OFFSHORE PLATFORM

C. S. Li[*], C. S. Yang[†], Nicholas G. Dagalakis[‡], and William Messick
Mechanical Engineering Department
University of Maryland
College Park, MD   20742

The purpose of this investigation was to determine the dynamic similitude
laws between a prototype offshore platform and its scale model and to in-
vestigate the accuracy of these laws and the effects of practical modeling
assumptions with the use of finite element dynamic models of the platform
and model. Dynamic similarity in a model experiment requires that model
and prototype be geometrically and kinematically similar and that the
loading be homologous in location and scaled appropriately in magnitude.
In order to derive the scaling parameters for the modeling of the offshore
platform, deep cantilever beam equations with hydrodynamic loading similar
to the one acting on a circular cylindrical pile were used. Eleven scal-
ing parameters were obtained for the dimensional analysis and from these
parameters eight dimensionless groups and corresponding scaling equations
were derived. The results of this analysis was applied to the design of
an 1:13.8 scale model of an existing four legged oil platform. The accu-
racy of the dynamic similitude analysis was investigated with finite
element computer models of both the prototype and the 1:13.8 scale model.
Dynamic characteristics of the prototype like eigenvalues, mode shapes and
transient response were compared with those of the model, and the influence
of the degree of detail of the finite element model on these characteristic
responses was determined. A study of the effect of approximations in the
model designs to exact scaling requirements indicated that if cost con-
siderations in model fabrication dictate the use of stock piping and
materials, then all of the response parameters of the model cannot be
directly scaled to obtain prototype response. One needs to combine scal-
ing laws, model response measurements, and finite element modeling in order
to obtain a reliable and relatively inexpensive method for designing better
offshore platforms.

INTRODUCTION

The high cost and sophistication of today's
offshore oil platforms increases the necessity
for accurate modeling techniques. The objective
of our work was to utilize finite element model-
ing to identify the effects of some commonly
made approximations in the construction and
testing of models of offshore platform designs.

In Section I of this paper, the appropriate
laws for the scaling of an offshore platform are
derived and it is shown that for exact scaling
the designer must satisfy one very difficult
scaling law relating the moduli of elasticity and

densities of the model and prototype platforms.
If the modulus of elasticity of the model mate-
rial is the same as the prototype material,
then the model material density must be λ times
the prototype material density, where λ is the
scaling ratio ℓ_p/ℓ_m. For any reasonable value
of λ, the model density requirement is im-
possible to satisfy because of material
unavailability.

Another difficulty in the construction of
scaled structures is the availability of struc-
tural members which are exact replicas of the
corresponding prototype members. For the
particular model that was being investigated,
stock steel tubes with the proper external
diameter and cross sectional areas required by
the scaling laws were not available. Since
the order of special size steel tubes for the
application was prohibitively expensive, a model-
ing compromise was made. Since the main objective
of the work was to study the dynamic

[*] Professor, National Taiwan University

[†] Professor, Mechanical Engineering Department,
University of Maryland

[‡] Assistant Professor, Mechanical Engineering
Department, University of Maryland

characteristics of the offshore platform, it was decided to select the dimensions of the steel tubes such that the total moment of inertia about a horizontal axis for the model and prototype satisfy the corresponding scaling law. This scaling causes a discrepancy in stress scaling.

To compare the dynamic response characteristics of the model and prototype structures, finite element models were developed. The prototype and model under investigation and the model test results are described in Section II.

A simple NASTRAN beam model was developed and is described in Section III of the paper. After the first experimental data showed that this finite model was not accurate enough, a NASTRAN space frame model was developed and it is discussed in Section IV. In order to investigate the errors introduced by modeling approximations four different finite element models were used to obtain predicted dynamic response characteristics.

I. SIMILITUDE ANALYSIS

For dynamic similarity in a model experiment, the requirements are that the model and prototype be geometrically and kinematically similar and that the loading be homologous in location and scaled appropriately in magnitude. Geometric similarity requires that the model have the same shape as the prototype and that all linear dimensions of the model be related to the corresponding dimensions of the prototype by a constant scale factor. Kinematic similarity of two elastic bodies requires that the rate of change of generalized displacement at corresponding points in the two bodies are in the same direction and related in magnitude by a constant scale factor. Dynamic forces on the two bodies at corresponding points must be parallel and related in magnitude by a factor at similar times. The similar times are related by a scale factor. The test conditions must be estimated so that all important forces are related by the same scale factor between two elastic bodies. When dynamical similarity exists, data measured in a model test may be related quantitatively to conditions in the prototype.

In order to insure dynamic similarity or similitude, the dimensionless groups relating the variables must be the same for both the model and the prototype. One way of obtaining the relevant dimensionless groups is to use The Buckingham Pi Theorem. This method is particularly useful if the differential equations governing the phenomenon are unknown. Success with this method depends upon the insight of the investigator in selecting the variables affecting the problem. If one of the important variables is left out, correlation of the data will be impossible. A more reliable method of obtaining the dimensionless groups utilizes the differential equations describing the phenomena, if they are known. These may be

non-dimensionalized and the resulting non-dimensional coefficients of the terms will be the non-dimensional groups.

If the differential equations of a structural dynamics problem are not known one may start by considering an equation of the form

$$\sigma = F(R, t, \rho, \nu, E, a, g, \ell, P) \qquad (1)$$

relating all physical quantities of the problem [1, 2, 3]. Forming the proper dimensionless groups between the physical quantities one has

$$\frac{\sigma}{E} = f\left[\frac{\bar{R}}{\ell}, \frac{t}{\ell}\sqrt{\frac{E}{\rho}}\frac{a}{g}, \frac{g\ell\rho}{E}, \frac{P}{E\ell^2}, \nu\right] \qquad (2)$$

To assure dynamic similitude one must ensure that the dimensionless groups of equation (2) have the same value for both the model and the prototype, but this is difficult if not impossible, because of practical considerations. The main difficulty comes from $\frac{g\ell\rho}{E}$ dimensionless group term, which contains the gravitational constant g. Assuming g is constant then the following requirement must be satisfied:

$$\frac{(E/\rho)_{\text{prototype}}}{(E/\rho)_{\text{model}}} = \frac{\ell_{\text{prototype}}}{\ell_{\text{model}}} \text{ or } \left(\frac{E}{\rho}\right)_r = \ell_r \qquad (3)$$

where the subscript r refers to the ratio of the the prototype to model quantities.

Relationship (3) means that the use of prototype material for the construction of a true replica model is impossible. If for example steel tubes are used for the construction of the model platform and the same modulus of elasticity E is maintained then the density of the model material must be:

$$\rho_{\text{model}} = \rho_{\text{prototype}} \frac{\ell_{\text{prototype}}}{\ell_{\text{model}}} \qquad (4)$$

Since the maximum size of the model structure is dictated by the size of available testing facilities and ℓ_r cannot be less than 15 to 10 we see that ρ must be 10 to 15 times the density of the steel prototype material. Materials which have a lower modulus do not have the required density.

From the rest of the dimensionless products in equation (2), assuming the same modulus of elasticity for model and prototype the following scaling laws [4, 5, 6, 7] must be satisfied along with the density law (eq (4)):

$$t_p = \sqrt{\lambda}\, t_m, \text{ (Time Scaling Law)} \qquad (5)$$

$$P_p = \lambda^2 P_m, \text{ (Force Sacling Law)} \qquad (6)$$

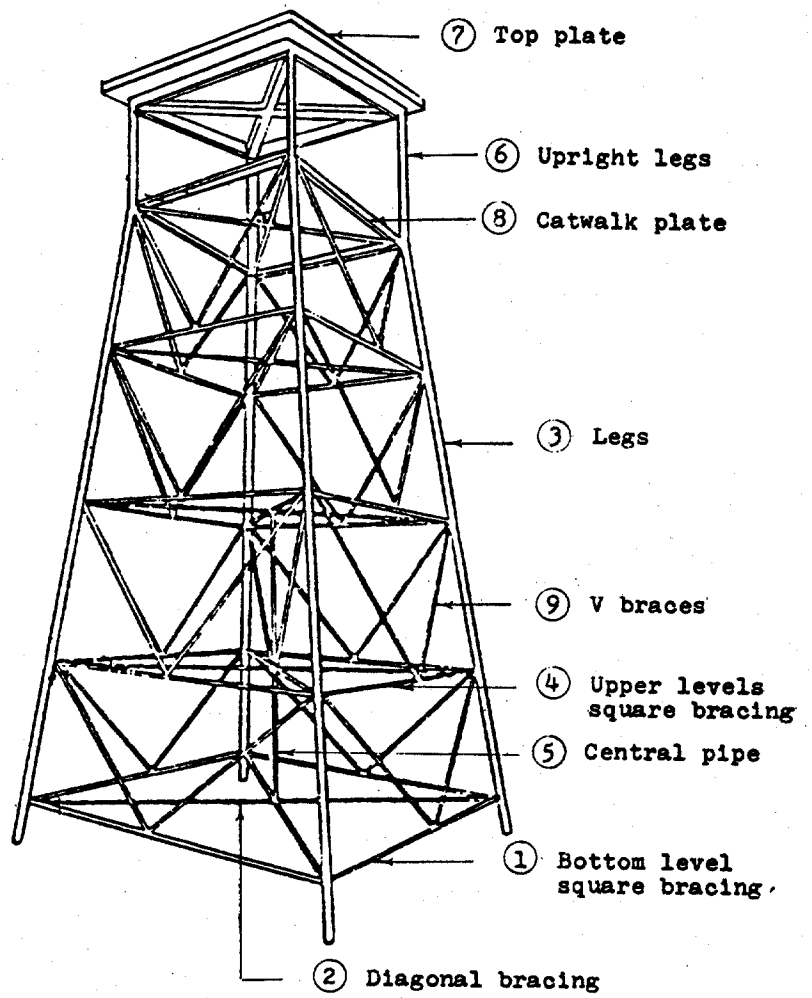$$\sigma_p = \sigma_m, \text{ (Stress Scaling Law)} \qquad (7)$$
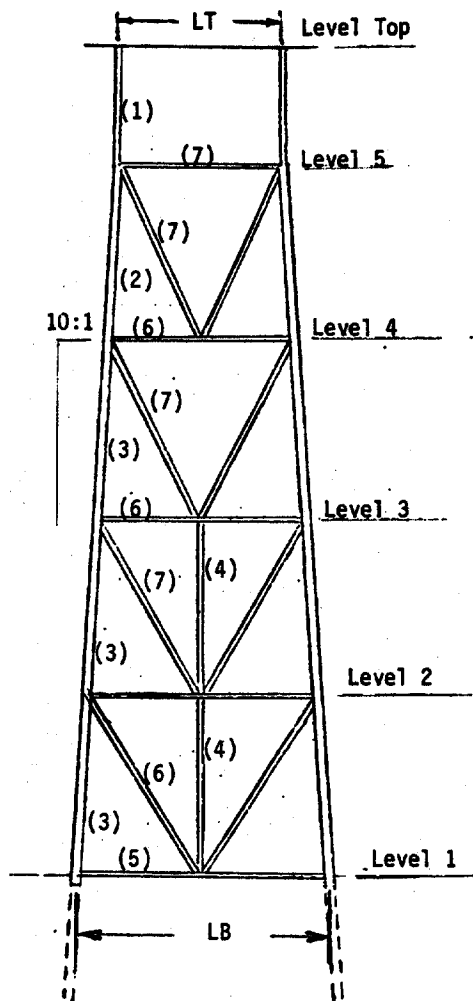
196

- (7) Top plate
- (6) Upright legs
- (8) Catwalk plate
- (3) Legs
- (9) V braces
- (4) Upper levels square bracing
- (5) Central pipe
- (1) Bottom level square bracing.
- (2) Diagonal bracing

FIGURE 2 - SCALE MODEL OF OFFSHORE PLATFORM

LT → Level Top

(1)

(7) Level 5

(7)

(2)

10:1 (6) Level 4

(7)

(3)

(6) Level 3

(7) (4)

(3)

Level 2

(4)

(6)

(3)

(5) Level 1

LB

Dimension of Segments:

(1) $30"^{\phi} \times 3/4"$ pL.

(2) $34\ 1/2"^{\phi} \times 3/4"$ pL.

(3) $34"^{\phi} \times 3/4"$ pL.

(4) $12\ 3/4"^{\phi} \times 49.6$ lbf/ft.

(5) $18"^{\phi} \times 82$ lbf/ft.

(6) $16"^{\phi} \times 73$ lbf/ft.

(7) $14"^{\phi} \times 63$ lbf/ft.

Materials:

A-36 Gas-pipe Steel

Height of Levels: H_i

H_1	0.00'
H_2	33.00'
H_3	62.02'
H_4	90.04'
H_5	116.04'
H_{Top}	155.02'

Top and Bottom Widths:

LT	40.0'
LB	65.6'

FIGURE 3 - PROTOTYPE DETAILS
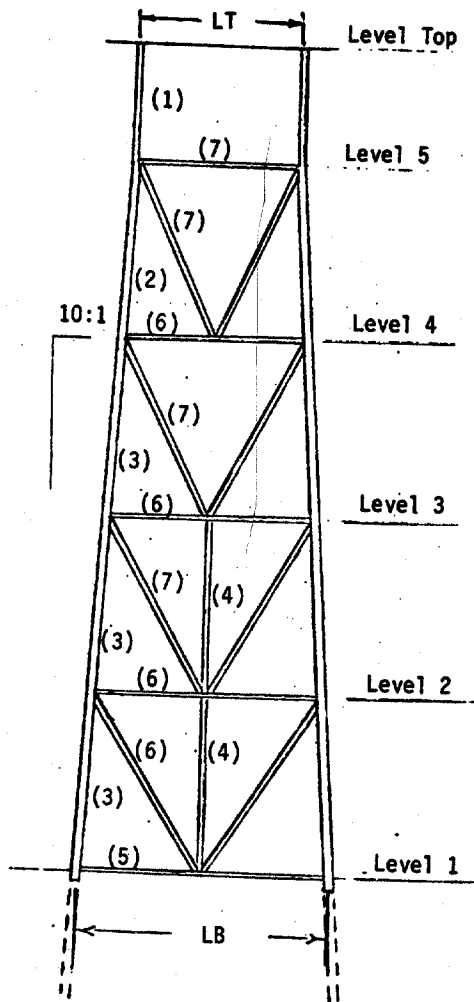
Dimensions of Segments:

1. $2"^{\phi}$ - B.W. Ga. 20
2. $2"^{\phi}$ - B.W. Ga. 20
3. $2"^{\phi}$ - B.W. Ga. 20
4. $9/16"^{\phi}$ - B.W. Ga. 20
5. $3/4"^{\phi}$ - B.W. Ga. 17
6. $3/4"^{\phi}$ - B.W. Ga. 18
7. $3/4"^{\phi}$ - B.W. Ga. 18

Materials:

ASTM A513-70 and QQT-7-830A
By RYERSON

Heights of Levels:

H_1	0.00'
H_2	2.39'
H_3	4.57'
H_4	6.53'
H_5	8.41'
H_{Top}	11.23'

Top and Bottom Widths:

LT   2.899'

LB   4.750'

FIGURE 4 - MODEL PLATFORM DETAILS FOR 13.8 SCALE FACTOR

201

Grid Point Numbers | Grid Point Locations

	Prototype	Model

NASTRAN Element
    Types   CONM 2 • 1   TOP PLATE   (1860.2)   (134.8)
CBAR elements
                        • 2   (1704.3)   (123.5)

                        • 3   (1548.4)   (112.2)

            CONM 2 • 4 – LEVEL 5   (1392.4)   (100.9)

                        • 5   (1236.5)   (89.6)

$(I + 1)^{th}$
element CONM 2 • 6 – LEVEL 4   (1080.5)   (78.3)

I^{th} element
                        • 7   (471.5)   (70.4)
$(I - 1)^{th}$
element   • 8   (862.5)   (62.5)

            CONM 2 • 9 – LEVEL 3   (756.2)   (54.8)

                        •10   (634.8)   (46.0)

                        •11   (516.1)   (37.4)

            CONM 2 •12 – LEVEL 2   (396.1)   (28.7)

                        •13   (263.6)   (19.1)

            X   •14   (132.5)   (9.6)
                    •15
            Y ←///// – LEVEL 1   (0.0)   (0.0)

                    Z

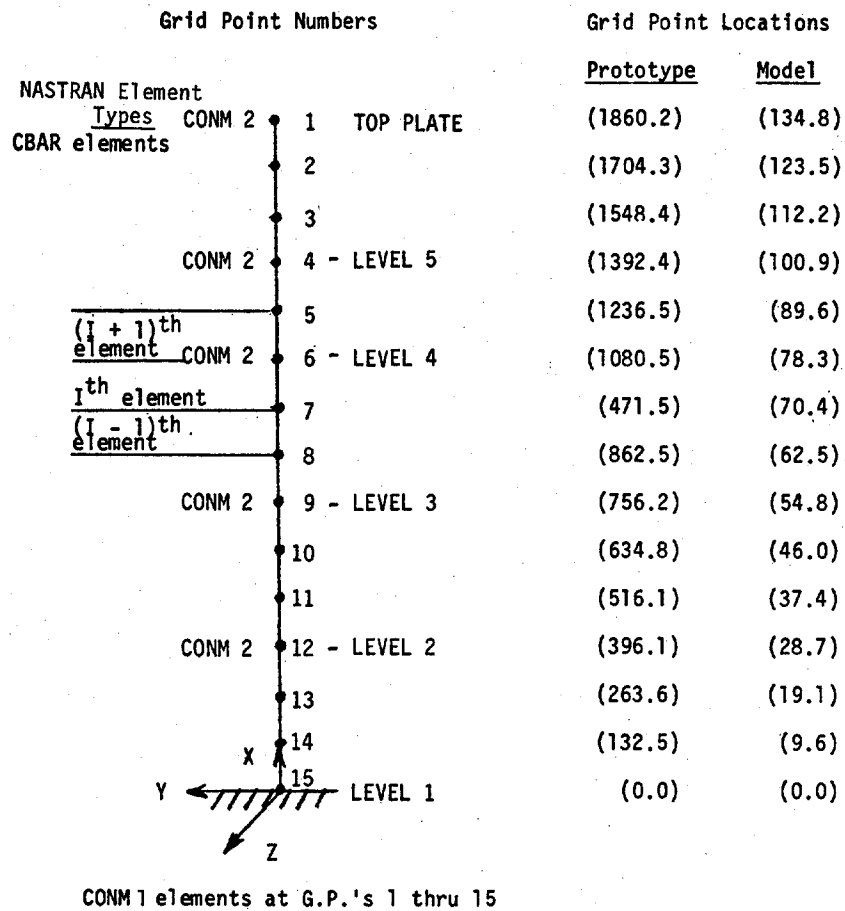CONM 1 elements at G.P.'s 1 thru 15

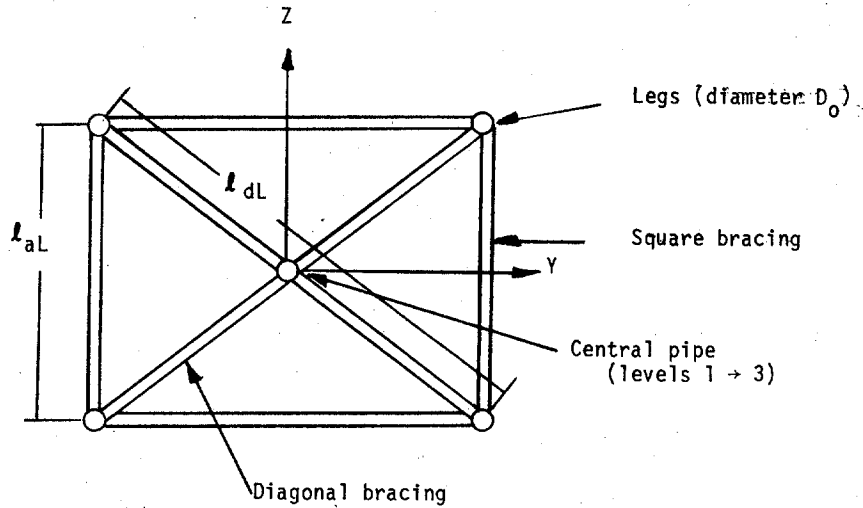FIGURE 5 – FINITE ELEMENT MODELS

202

FIGURE 6 – HORIZONTAL MEMBER ARRAY AT THE L^{TH} LEVEL

B. Natural Frequency Results

The model described in the previous subsection of this report was put into NASTRAN Rigid Format 3 for a normal mode analysis using the Givens method of solution.

Table 2 summarizes some of the results of the NASTRAN beam model investigation. The first 10 natural frequencies of the finite element models of the prototype are compared with the corresponding natural frequencies of the real model.

According to the scaling laws derived in Section I for the case where $E_p = E_m$ and $\rho_p = \rho_m$, f_m/f_p must be λ. As seen in Table 2, the finite element modeling of the prototype and fabricated (real) model indicate that there is considerable modeling errors for some frequencies. However, the absolute values of the errors obtained from the NASTRAN results are not in agreement with the measured model fundamental frequency.

TABLE 2

NASTRAN Beam Model Results

Nat. Frequency – (Hz)

Prototype	Real Model	f_m/f_p	Error
2.08	25.25	12.13	-12.1%
2.43	28.93	11.90	-13.7%
7.98	96.40	12.08	-12.4%
9.93	124.21	12.50	- 9.4%
12.37	154.95	12.52	- 9.2%
20.80	270.84	13.02	- 5.6%
26.25	337.68	12.86	- 6.8%
31.23	339.44	12.93	- 6.3%
34.20	412.87	12.07	-12.5%
34.71	533.45	15.36	+11.3%

IV. NASTRAN SPACE FRAME MODEL

The NASTRAN beam model was the first attempt to get an estimate of the error in satisfying the scaling laws between the prototype and the model platform. The computer model was simple and relatively inexpensive to run even for long dynamic response simulations.

As soon as the model platform was completed though it became apparent that this approximate model was giving results, which were off by as much as 100% to 300% of the actual measured data. For example the fundamental flexural mode frequency was measured to be 8 Hz, while the NASTRAN beam model predicted it to be 25 Hz. Furthermore the beam model was very crude and did not allow evaluation of the stresses of individual beam members.

For these reasons, NASTRAN space frame models were developed for the prototype and the real model platform (see Figure 7). Also, to investigate the error introduced by taking $E_p = E_m$ and $\rho_p = \rho_m$ a NASTRAN space frame model of the real model with scaled density $\rho_m = \lambda \rho_p$ was developed. To investigate the error resulting from not scaling the exact cross sectional geometry of the prototype beams in the real model, a NASTRAN space frame model of a prototype scaled up from the real model was developed.

Because there were a number of different model and prototype designs to be analyzed all with the similar configuration of four legs and vertical and horizontal diagonal bracing, a pre-processor program (GENER) was written to generate NASTRAN coordinate and connection cards (GRID and CBAR). The pre-processor program will automatically generate all the connectivity cards associated with all the piping of the platform except for the central pipe which is added by hand, with the option of connecting juncture points of the structure with one or two CBAR elements. Two CBAR elements were connected by platform juncture points for this study. Individual piping cross sectional area, mass, and moment of inertia properties are included in the model through the NASTRAN PBAR card. The grid point numbering sequence produced by the generator program is not banded, so after the central piping and plate elements are added to the finite element model, BANDIT is used to obtain sequenced grid point connectivity.

The results of the NASTRAN Rigid Format 3 (Normal Mode Analysis) computer runs are summarized in Tables 3, 4, and 5. Table 3 compares the natural frequencies of the prototype scaled up from the real model, with the model that has density properly scaled. Since these two hypothetical models satisfy all the scaling laws (equations (4) to (10)), the frequency ratio relationship $f_m/f_p = \sqrt{\lambda} = \sqrt{13.8} = 3.71$ should be satisfied with great accuracy, and as shown in

Table 3, there is excellent agreement between the results from the two finite elements.

Table 4 compares the natural frequencies of the prototype scaled up from the real model to those obtained from the finite element model of the real platform. Since these models assume equal moduli and material densities and satisfy all other scaling laws, then according to equation (26), the frequency ratio of $f_m/f_p = \lambda = 13.8$ should be satisfied. The errors for the first four modes are less than two percent. Also from Table 4, it can be seen that the agreement of the finite element model fundamental frequency of 8.52 Hz and the measured frequency of 8 Hz for the constructed real model is good.

Table 5 compares the NASTRAN natural frequencies of the real prototype with the real model. The frequency ratio relationship of $f_m/f_p = \lambda = 13.8$ is not well satisfied. This error is a direct result of the modeling criterion that was used in the model design and construction; that is, since stock tubing was not available in sizes which directly scale from the real prototype pipe sizes, then available piping would be used to scale the total cross sectional area of the vertical members and the bending moment of inertia produced by the vertical legs.

To investigate the scaling accuracy of the dynamic response variables, the NASTRAN finite element models were loaded with a square pulse force applied at node A in the y direction as shown in Figure 7 to simulate a ship impact on an offshore platform. The amplitude of the pulse is F_o and its duration is T_o. Each of the above mentioned finite element models was run in NASTRAN Rigid Format 9 (Transient Response) to obtain the displacement, acceleration and stress at critical points as a function of time. For the offshore platform finite element model, F_o and T_o were selected to be 10^6 lbs and 1.38 seconds, respectively. Using the appropriate scaling law, equations (5), (6), (21), or (22), the following loadings in Table 6 were obtained.

Typical dynamic responses at point C of the space frame model in Figure 7 are shown in Figure 8 through 13. The acceleration in the Y direction at point C in Figure 7 for the real model, the model with scaled density, and the prototype scaled up from the real model are shown in Figures 8, 9, and 10, respectively. The time scales in these figures are scaled according to the appropriate scaling law, and as can be seen both the timing and scaled magnitude of the response agrees excellently. The real model acceleration should be λ times the scaled-up prototype. The displacements, as would be expected, also show excellent agreement. This implication of these results are that the finite element models demonstrate that the scaling laws are correct.

204

Natural Frequencies of NASTRAN Space Frame Models (in Hz)

TABLE 3

Prototype Scaled Up From Real Model	Model with Scaled Density	f_m/f_p (Should be $\sqrt{\lambda} = 3.71$)	Error
.61	2.29	3.75	+1.0%
.61	2.29	3.75	+1.0%
.89	3.32	3.73	+0.5%
2.34	8.70	3.71	+0.0%
2.76	10.28	3.72	+0.2%
2.76	10.28	3.72	+0.2%

TABLE 4

Prototype Scaled Up From Real Model	Real Model	f_m/f_p (Should be $\lambda = 13.8$)	Error
.61	8.52	13.96	+1.2%
.61	8.52	13.96	+1.2%
.89	12.33	13.85	+0.3%
2.34	32.81	14.02	+1.6%

TABLE 5

Prototype	Real Model	f_m/f_p (Should be $\lambda = 13.8$)	Error
.77	8.52	11.06	-19.8%
.77	8.52	11.06	-19.8%
1.08	12.33	13.07	-17.2%
2.51	32.81		- 5.2%

TABLE 6

Dynamic Loading Parameters

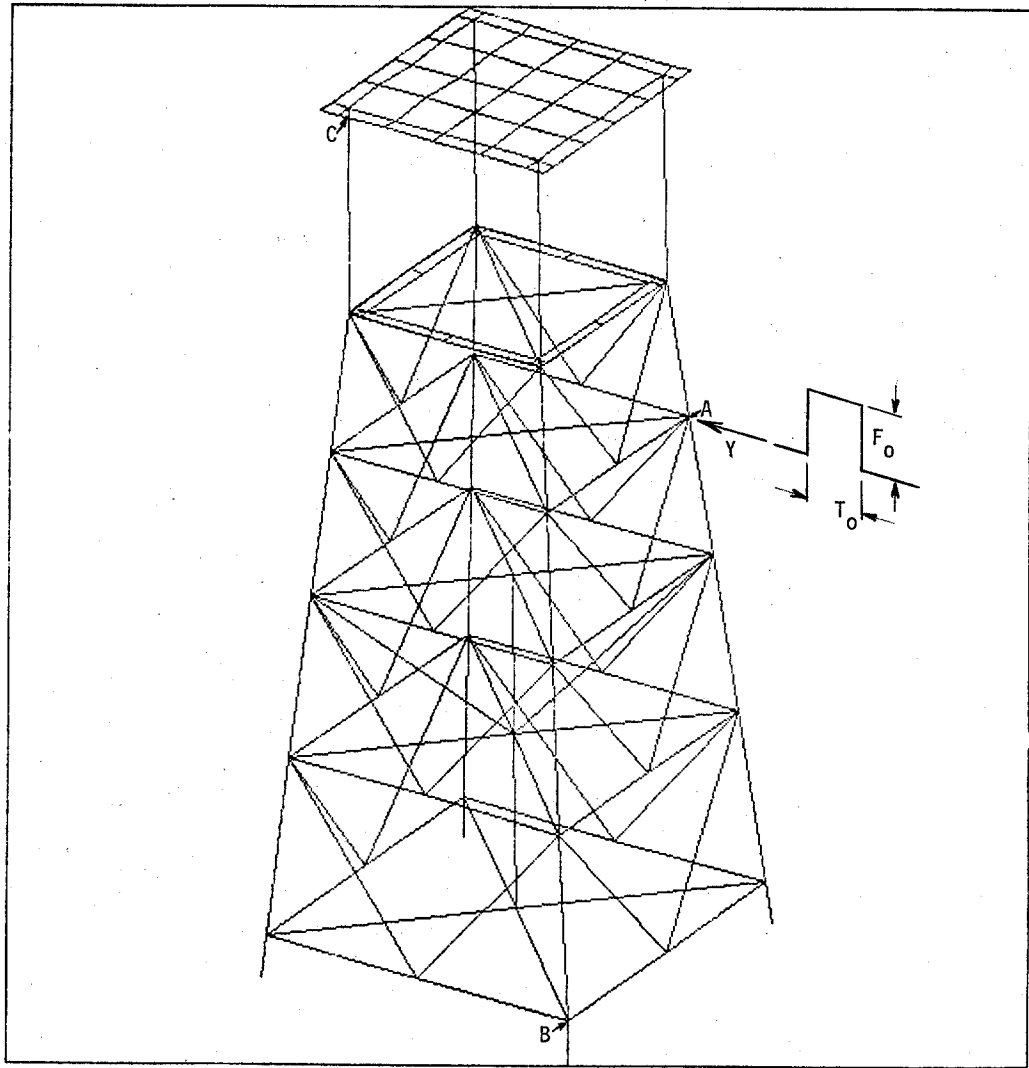|	Real Prototype	Real Model	Model With Scaled Density
F_o (lbs) 10^6		5,251	5,251
T_o (See) 1.38		0.1	0.371

FIGURE 7 - COMPUTER GENERATED PLOT OF NASTRAN FINITE ELEMENT SPACE FRAME MODEL
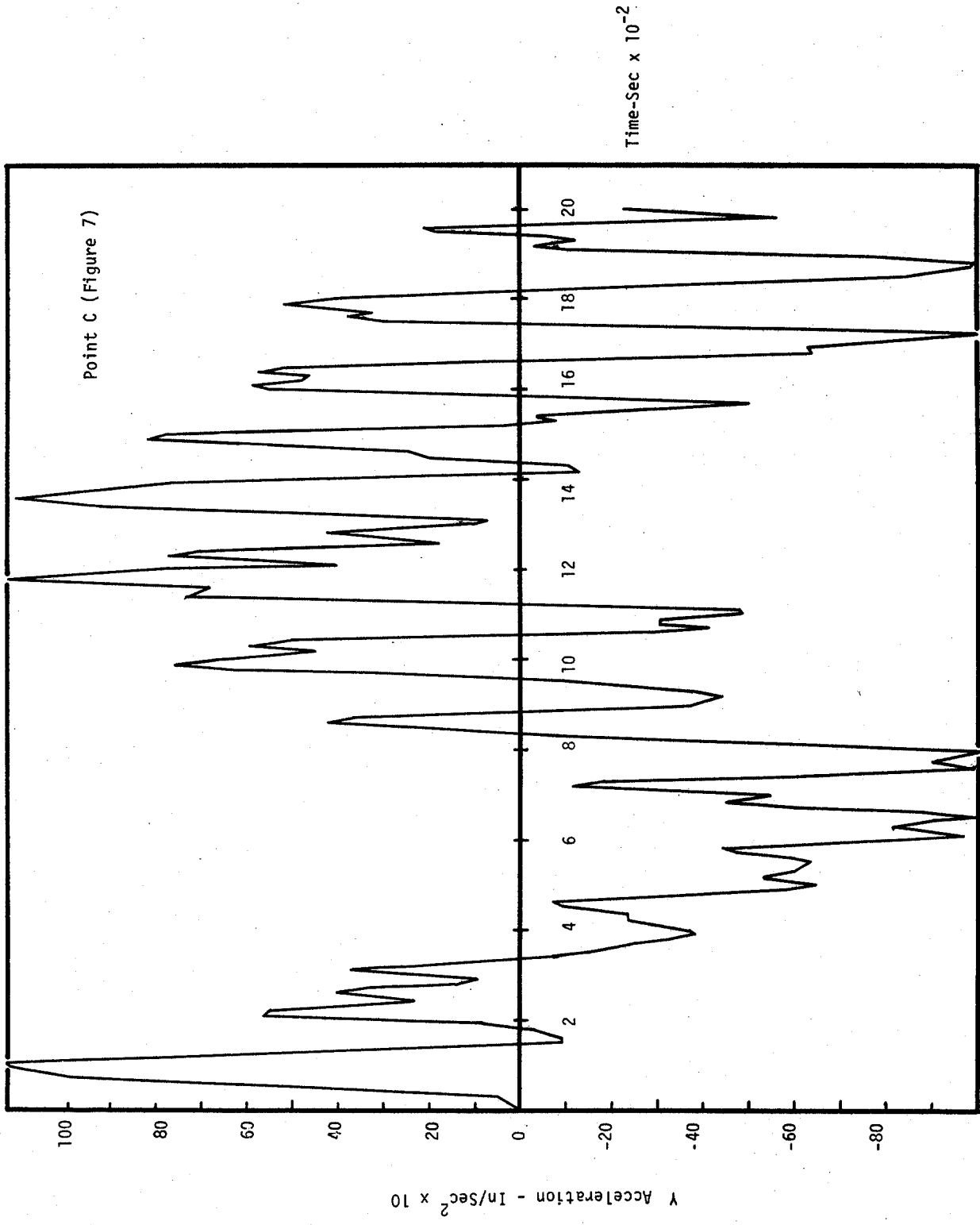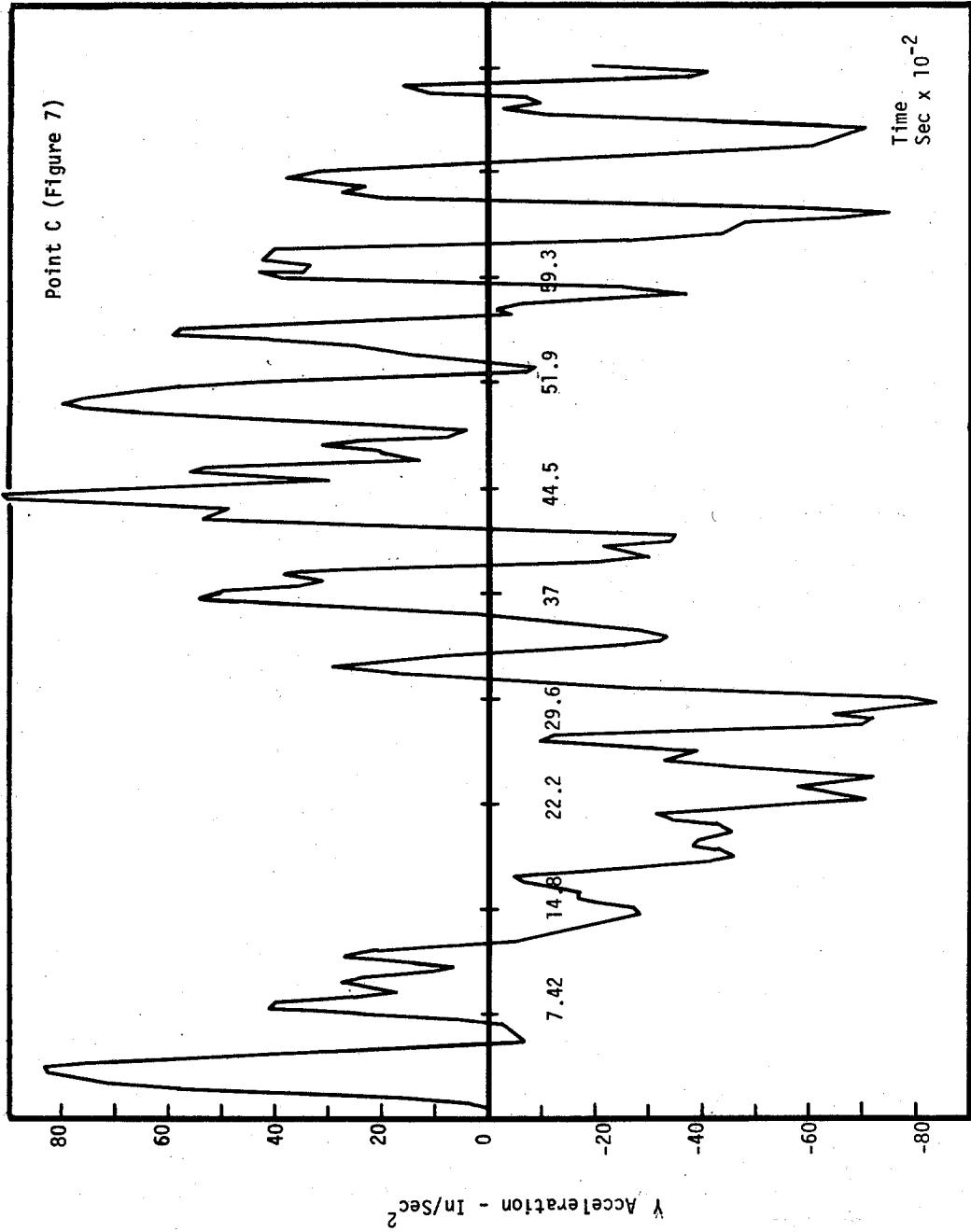
FIGURE 8 - REAL MODEL

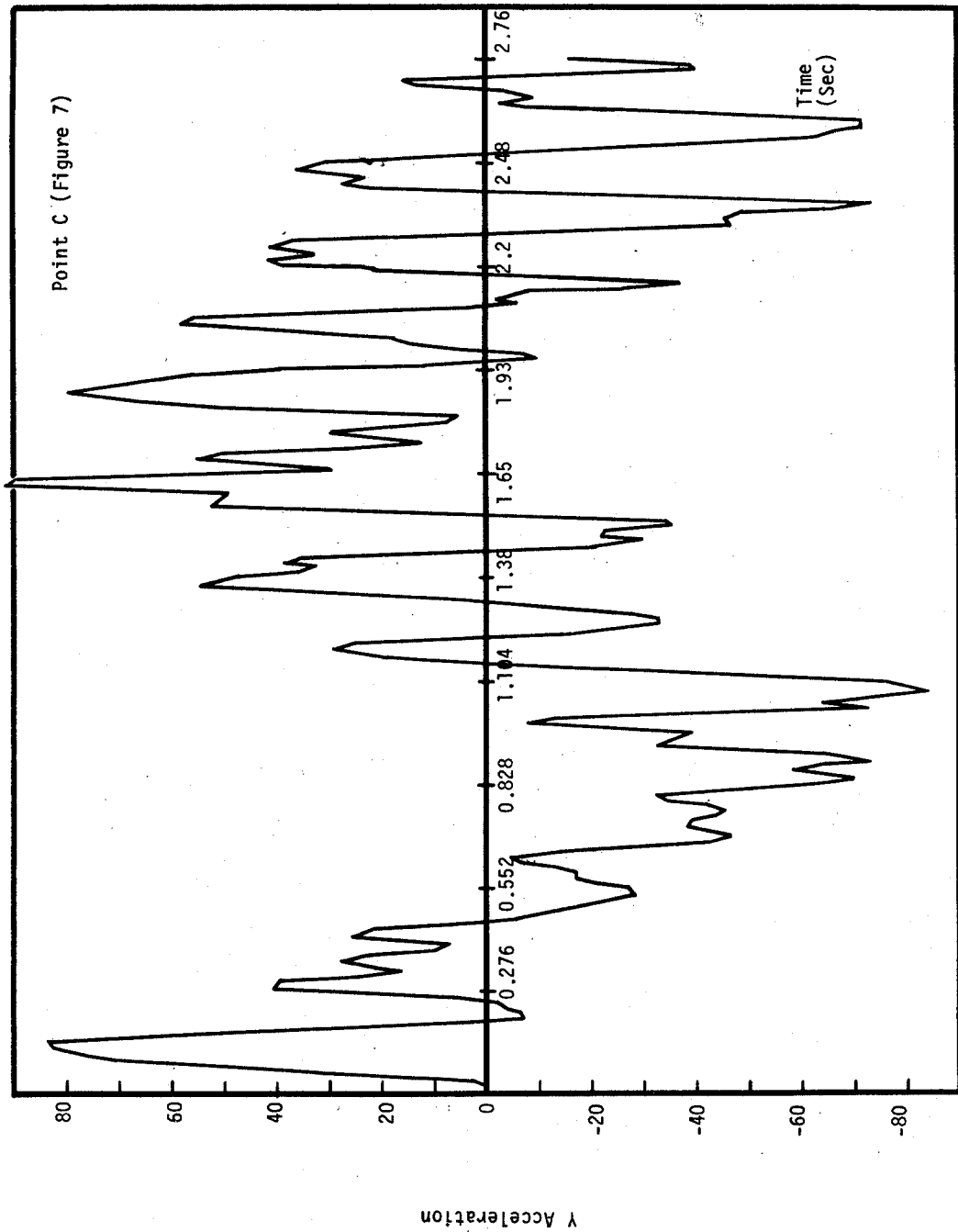FIGURE 9 - MODEL WITH SCALED DENSITY

FIGURE 10 - PROTOTYPE SCALED UP FROM REAL MODEL

In contrast to the excellent agreement of these three previously mentioned models, the acceleration response of the prototype is shown in Figure 11. As compared to Figure 10, the phasing of the acceleration is much in error and this is a direct result of the difference in natural frequency response of these two structures. Although the phasing of the real and scaled-up from model prototypes is different, the absolute magnitude of the acceleration is close.

According to equation (7) and (23), stress should scale equally whether density is appropriately scaled or not. The results were obtained on the prototype scaled up from the real model, the real model, and the model with scaled density demonstrated equal stresses at equal scaled time. A big discrepancy was obtained again in the response of the real prototype. Shown in Figures 12 and 13 are the bending stresses at the outside surface of the piping at location B in Figure 7 for the prototype scaled up from the real model and the real prototype. The phasing of the response is not the same because of the previously mentioned natural frequency discrepancies, but instead of equal maximum stresses in both structures the real prototype stress level is one half that of the prototype scaled up from the real model. This error is a direct result of the properties of the piping on each structure. Shown in Table 7 are the properties of the tubing at location B for each structure.

Since the bending stress is

$$\sigma = \frac{M\left(\frac{D_o}{2}\right)}{I} \tag{28}$$

then

$$\frac{\sigma_p\big|_{real}}{\sigma_p\big|_{scaled\ up}} = \frac{\sigma_R}{\sigma_S} = \frac{M_R}{M_S} \frac{\left(D_o\right)_R}{\left(D_o\right)_S} \frac{I_S}{I_R} \tag{29}$$

Using the properties of Table 7 in equation (29) yields

$$\frac{\sigma_R}{\sigma_S} = .43 \frac{M_R}{M_S} \tag{30}$$

Even though the static moments are equal for the two structures, the dynamic moments, M_R and M_S won't necessarily be the same because of the different dynamic response of the structures. However they should be close in magnitude and thus, from the difference in tubing properties of the two structures, the stress in the real prototype would be expected to be approximately 43 percent of that in the prototype scaled up from the real model at point B, and this is in close agreement with the NASTRAN results.

V. CONCLUSIONS

Space frame finite element models have been used to substantiate two sets of derived scaling laws for dynamic response of offshore platforms. One set of scaling laws would be satisfied if every member of the model structure were exactly scaled down in dimensions from the prototype structure and the model material modulus was maintained while the density was appropriately scaled up. The other set was derived with the exact same assumptions except that the prototype and model densities are equal. The effects of the modeling differences are that the phasing of the dynamic response of the two different models differ by a $\sqrt{\lambda}$ factor and that acceleration magnitudes of prototype and model are the same when densities are scaled, whereas, the acceleration magnitude differ by a factor of λ when prototype and model densities are the same. With either set of scaling laws, dynamic stresses in both model and prototype are equal and to ensure equal total stresses, the static stresses must be equal which is satisfied by scaling model density.

Two difficulties are encountered in exactly satisfying the scaling laws for offshore platforms: one is obtaining the correct model material density and the other is obtaining model tubing which is an exact scaled-down size of the prototype piping. For practical scaling ratios, the required model material density is very high. For scaled down tubing, it is very unlikely that the correct inside and outside diameters can be obtained in stock sizes. Manufacturing the correct scaled down replica would be prohibitively costly if not impossible

TABLE 7

Tubing Properties in Structures at Location B (Figure 7)

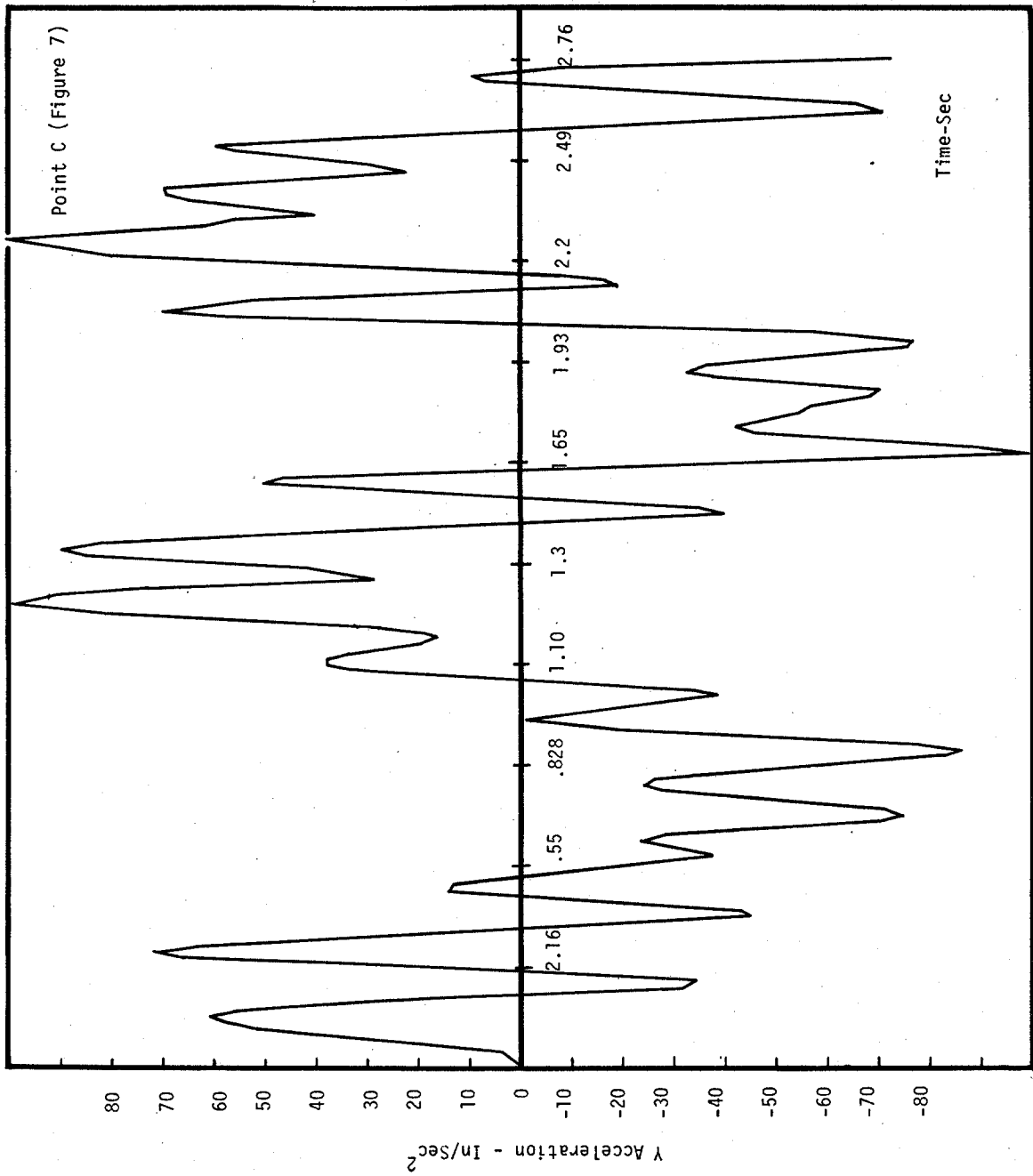| Property	Prototype Scaled Up From Model	Real Prototype
Distance to outside surface $\left(\frac{D_o}{2}\right)(in)$	13.8	17.0
Cross sectional area (in^2)	41.1	78.3
Moment of inertia (in^4)	3,783	10,832

FIGURE 11 – PROTOTYPE

211
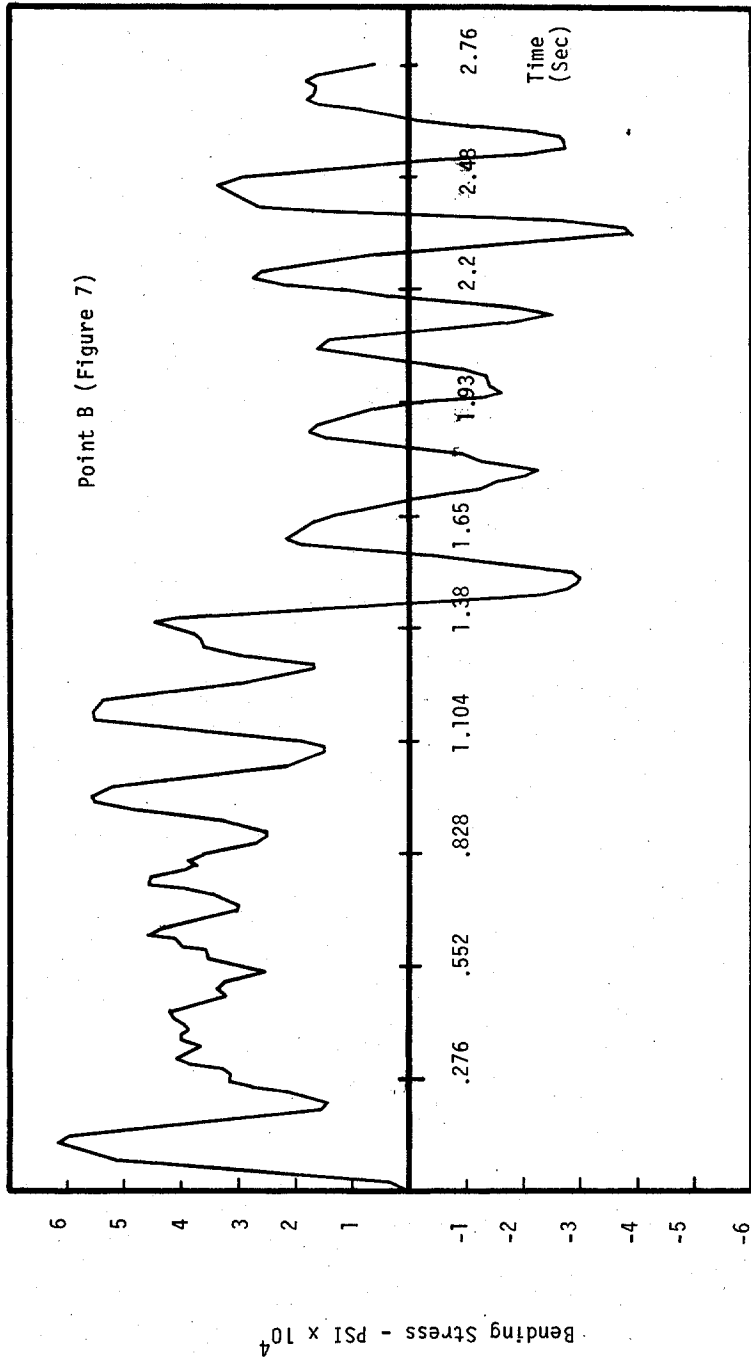
FIGURE 12 – PROTOTYPE SCALED UP FROM REAL MODEL

Point B (Figure 7)

Bending Stress - PSI x 10^4

TIME-SEC

.276   .55   .828   .11   .138   .165   .193   .249   .276
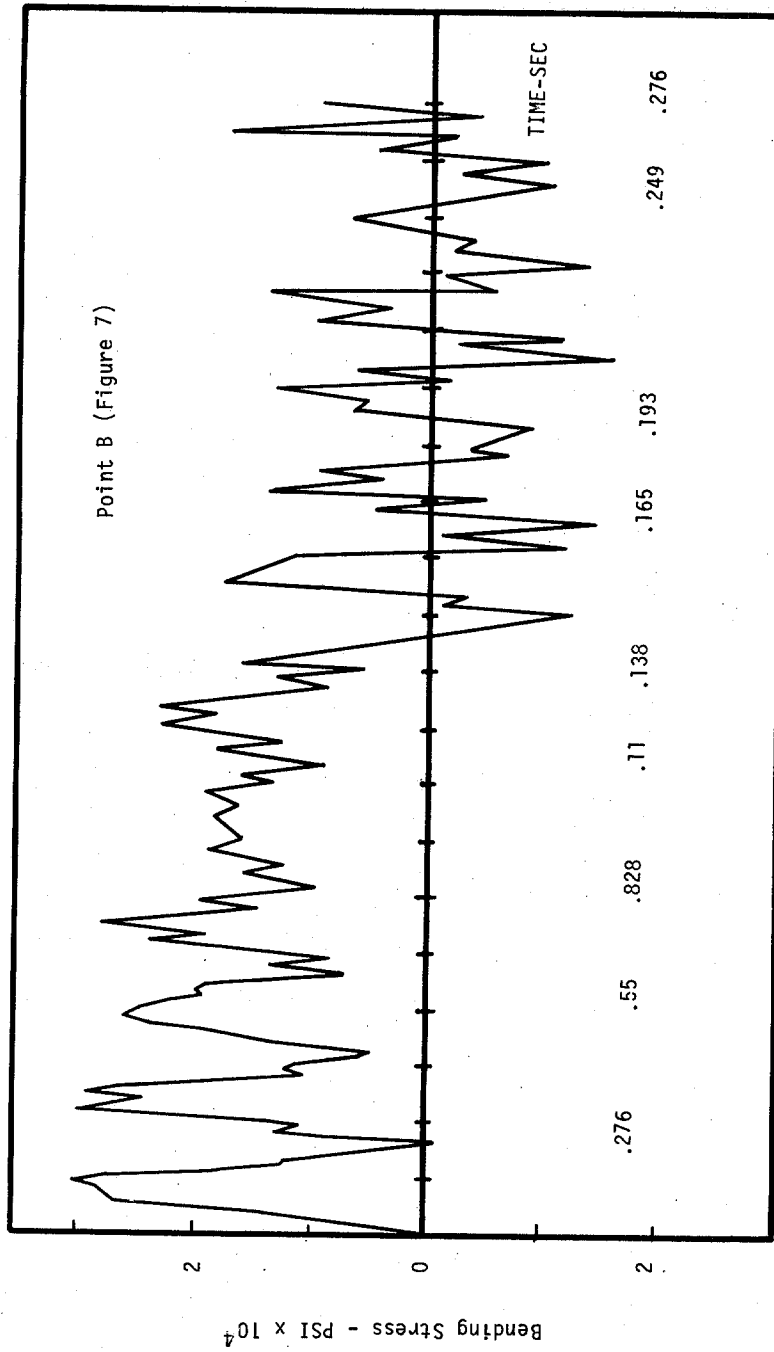
FIGURE 13 - PROTOTYPE

213

because of minimum gauge requirements or buckling problems.

The best model design for an offshore structure can only be obtained by selecting stock tubing to satisfy scaling laws as nearly as possible and then using finite element modeling of the proposed model and prototype to determine if the dynamic response of the two satisfy scaling laws. If the proposed model doesn't scale accurately enough then other tubing should be selected and modeling done until sufficiently scaling accuracy is obtained.

ACKNOWLEDGEMENTS

REFERENCES

1. H. Krawinkler, R.S. Mills, P.D. Moncarz, "Scale Modeling and Testing of Structures for Reproducing Response to Earthquake Excitation", John A. Blume Earthquake Engineering Center, Stanford University, 1978.

2. P. Le Corbeiller, A.V. Lukas, "Dimensional Analysis", Appleton-Century-Crofts Publishing Co.

3. W.J. Duncan, "Physical Similarity and Dimensional Analysis", Edward Arnold and Co., Publ.

4. H.A. Becker, "Dimensionless Parameters Theory and Methodology", Applied Science Publishers Ltd.

5. A.A. Gukhman, "Introduction to the Theory of Similarity", Academic Press Publ.

6. P.W. Bridgman, "Dimensional Analysis", Yale Univ. Press.

7. C.M. Focken", Dimensional Methods and Their Applications", Edward Arnol- and Co. Publ.

NOMENCLATURE

A	cross sectional area
A_L, A_C	cross sectional area of a leg and central pipe, respectively
a	acceleration
D_o	outside diameter of the leg
E	modulus of elasticity
f	frequency
G	shear rigidity
g	gravitational constant
I	moment of inertia
I_L, I_C	mass moment of inertia about a leg and a central pipe, respectively
K'	shear area coefficient
ℓ	length
ℓ_{aI}	center to center distance between legs of Ith BAR element
ℓ_{dL}	center to center diagonal distance between legs at level L
ℓ_I	length of Ith BAR element
M	bending moment in beam
m	mass of beam per unit length
P	applied load
p	load pressure
$\bar{p}$	lateral load per unit length of beam
r	radius of gyration of beam cross section
t	time
$\bar{V}$	end shearing force
x	distance along length of beam

Greek Letter Symbols

α	angle of rotation of the beam cross section from its original vertical position (without shear distortion)
β	angle of shear distortion of the beam cross section, β will reduce the slope of the elastic curve of beam axis
λ	ratio of prototype to model length
Π_i	dimensionless group i
ρ	density
σ	stress

Subscripts

m	denotes model
p	denotes prototype
r	indicates ratio of prototype to model quantities

APPENDIX I

Model Design

The offshore platform structure under consideration for this study is shown in Figure 2 with details in Figure 3. It is a 4 pile jacket design with a deck 155 feet above the ocean bottom 105 feet of water. The model scaling was obtained by consideration of commercially available structural members for the model platform construction.

The four legs of the prototype are made

of $34\frac{1}{2}''$ O. D. x $\frac{3}{4}''$ plate pipe spaced $65'$ $7\frac{3}{16}''$ apart and the central pipe is $12\frac{3}{4}''$ O. D. x $\frac{3}{8}''$ plate. The total cross sectional areas of these members is thus

$$A_p = 4(A_L)_p + (A_c)_p = 175.39 \text{ in}^2 \quad (A.1)$$

Where A_L, A_c is the cross sectional area of the leg and central pipe respectively.

The moment of inertia of these members about the Z axis in Figure 6 is

$$I_p = (I_c)_p + 4(I_L + A_L k_L^2)_p = 25.064(10^6) \text{ in}^4 \quad (A.2)$$

The model bending moment of inertia is

$$I_m = (I_c)_m + 4(I_L + A_L k_L^2)_m \quad (A.3)$$

The contribution of the moment of inertia of the central pipe, $(I_c)_m$, to the total moment of inertia of the model at the bottom, I_m, is small so it may be neglected. Substituting the scaling relationships $\frac{I_p}{I_m} = \lambda^4$, $\frac{A_p}{A_m} = \lambda^2$ from (13) and (17) into equation (A.2) yields

$$\lambda^4 + \left(\frac{A_L}{I_L}\right)_m \left(k_L\right)_p^2 \lambda^2 - \frac{I_p}{4\left(I_L\right)_m} = 0 \quad (A.4)$$

But

$$\frac{\left(A_L\right)_m}{\left(I_L\right)_m} = \frac{\left(A_L\right)_m}{\left(A_L\right)_m \cdot \frac{1}{16}\left(d_o^2 + d_i^2\right)_m}$$

$$= \frac{16}{\left(d_o^2 + d_i^2\right)_m} \quad (A.5)$$

Therefore

$$\lambda^2 = \sqrt{\left(\frac{1245799.55}{\left(d_o^2 + d_i^2\right)_m}\right)^2 + \left(\frac{6266065.29}{\left(I_L\right)_m}\right)}$$

$$- \frac{12945799.55}{\left(d_o^2 + d_i^2\right)_m} \quad (A.6)$$

Equation (A.6) is used to size the model columns and then the central pipe may be sized to satisfy the exact scaling equation. Using Ryerson carbon steel round mechanical tubing $2''$ O. D. by B. W. Ga. 20, the properties are

$$d_o = 2.0'' \quad (A.7)$$

$$d_i = 1.93''$$

$$\left(A_L\right)_m = 0.216 \text{ in}^2$$

$$\left(I_L\right)_m = .1043 \text{ in}^4$$

Substituting into equation (A.6) yields $\lambda = 13.64$. for the central pipe, the properties of Ryerson Carbon steel round mechanical tubing $\frac{9}{16}''$ O. D. by B. W. Ga. 20 are:

$$d_o = \frac{9''}{16} \quad (A.8)$$

$$d_i = .493''$$

$$\left(A_c\right)_m = 0.057 \text{ in}^2$$

$$\left(I_c\right)_m = 0.00199 \text{ in}^4$$

Then from (A.1) the scaling factor is:

$$\lambda = \sqrt{\frac{A_p}{A_m}} = \sqrt{\frac{175.39}{4(.216) + .057}} = 13.8 \quad (A.9)$$

Checking the moment of inertia scaling:

$$\sqrt[4]{\frac{I_p}{I_m}} = \quad (A.10)$$

$$\sqrt[4]{\frac{25.064(10^6)}{.002 + 4\left(.1043 + .216\left(\frac{393.6}{13.8}\right)^2\right)}} = 13.75$$

Thus a scaling factor of $\lambda = 13.8$ is chosen for the model.

The top deck of the platform was modeled as a uniform thickness plate which was sized in length according to the structural scaling factor λ and in thickness so that the weight is scaled according to the cube of λ. Similar scaling was done on the catwalk at level 5 of the platform. The resulting platform model is shown in detail in Figure 4.

DISCUSSION

Mr. Galef (TRW): I would think that the loads you were mostly concerned about would be the ones from starboard. If we ever had that model in the water the violation of the Froude law scaling that you had would seem to be completely unusable.

Mr. Dagalakis: The loadings that we have is wrong from the waves, is that the question?

Mr. Galef: Yes, that is correct.

Mr. Dagalakis:: And also from collisions. Sometimes the supply ship will collide with the offshore platform. The study that we did here was for that kind of load and occasionally we have collisions.